 CMES, vol.6, no.5, pp.431-439, 2004

A General Tangent Operator Procedure for Implicit Elastoplastic BEM Analysis

L.S. Miers and J.C.F. Telles[1]

Abstract: Most formulations involving the use of the so-called consistent elastoplastic tangent operator procedure, in boundary element analysis, have been presented taking in consideration only a J_2-type yield criterion, like von Mises. The present paper aims at bringing a general consistency concept to tangent operators obtained without yield criterion particularization, ready to be used in implicit schemes for elastoplastic BEM analysis. The ideas follows much of the second author's physically nonlinear implicit BEM solution procedures introduced in the 80's and is based on a Taylor series expansion of the true effective stress around an equivalent stress corresponding to the accumulated true stresses up to, but not including, the current increment taken to be "elastic". To illustrate the efficiency of the technique, some comparative results using different yield criteria are presented.

keyword: elastoplasticity, boundary elements, implicit algorithms.

1 Introduction

The first implementation of BEM to nonlinear analysis is due to Riccardella (1973) where a pure incremental solution scheme was used for inviscid plasticity problems obeying the von Mises yield criterion.

As pointed out by Telles (1985), until the mid eighties all the developed algorithms for BEM elastoplastic analysis were mostly based on explicit schemes, which had shown to be quite efficient until then. That work was the first to present implicit routines to solve elastoplastic problems by BEM and was continued by Telles and Carrer (1988, 1991 and 1994) Some improvements were made after that, mainly due to the use of modified tangent operators included in the previous implicit schemes and the most implemented ones are the so-called Continuum Tangent Operator (CON) and the Consistent Tangent Operator (CTO).

[1] COPPE/Univ. Fed. do Rio de Janeiro, RJ, Brazil – lsmiers@coc.ufjr.br, telles@coc.ufrj.br

Implicit CON BEM formulations have been presented by Telles (1985) and later by Jin, Runesson and Mattiasson (1989). It was also efficiently used in the analysis of large-strain viscoplastic problems by Mukherjee and Leu (1994). The CTO was brought to the BEM context by Bonnet and Mukherjee (1996) from a rate-independent plasticity FEM formulation presented by Simo and Taylor (1985). Details about the differences of CON and CTO can be found in Poon, Mukherjee and Bonnet (1998) and in Paulino and Liu (2001). However, all the CTO-based implicit schemes found in the literature were mostly based on a J_2-type yield criterion, such as von Mises', which is not generally well suited for all problems (e.g., soil or concrete). Additional applications on inelastic material behavior can be found in Okada, Rajiyah and Atluri (1990), Hatzigeorgiou and Beskos (2002) and Liu and Chang (2004).

The present work aims at introducing the concept of tangent operators, obtained without any kind of yield criterion particularization, to be used in implicit schemes for elastoplastic analysis by BEM. To illustrate the efficiency of the technique, some comparative results achieved with other methods are presented in the end.

2 BEM formulation for elastoplastic analysis

For the solution of general inelastic problems by the BE technique, a boundary integral equation can be obtained through weighted residual procedures or in the light of simple reciprocal statements as seen in Telles (1983). Herein, only its final form is shown (body forces are neglected for simplicity),

$$c_{ij}(\xi)\dot{u}_j(\xi) = \int_\Gamma u^*_{ij}(\xi,x)\dot{p}_j(x)d\Gamma(x) - \int_\Gamma p^*_{ij}(\xi,x)\dot{u}_j(x)d\Gamma(x) + \int_\Omega \varepsilon^*_{jki}(\xi,x)\dot{\sigma}^p_{jk}(x)d\Omega(x) \quad (1)$$

where Ω represents the domain of the body, Γ its boundary and c_{ij} is the usual free coefficient found in elastic

analysis. In addition, a dot can be associated with a pure incremental quantity for inviscid plasticity, and the following notation is used:

- u^*_{ij}, $p^*_{ij}$and ε^*_{jki}: displacement, traction and strain components at point x due to a unit concentrated load applied in "i" direction at point ξ (fundamental solution).
- $\dot{u}_j$, $\dot{p}_j$ and $\dot{\sigma}^p_{jk}$: displacement, traction and fictitious "plastic" stress increments (whose components are presented in Section 4) of the problem to be solved.

It is worth mentioning that Eq. (1) is meant to be valid for general 3D and 2D problems, provided subscripts are assumed to vary between 1-3 and 1-2 respectively.

Since in the case of material nonlinear analysis the constitutive equations are functions of the stress level at every point within the body, the computations of internal stresses is of great importance in the solution procedure. Therefore, the derivatives of Eq. (1), written for $\xi \in \Omega$, can be combined to represent the internal stress rates in the form

$$\dot{\sigma}_{ij}(\xi) = \int_\Gamma u^*_{ijk}(\xi,x)\dot{p}_k(x)d\Gamma(x) - \int_\Gamma p^*_{ijk}(\xi,x)\dot{u}_{jk}(x)d\Gamma(x) + \int_\Omega \varepsilon^*_{ijkli}(\xi,x)\dot{\sigma}^p_{kl}(x)d\Omega(x) + g_{ij}(\dot{\sigma}^p_{kl}) \quad (2)$$

where the last two terms introduce the fictitious "plastic" stress influence. It should be mentioned that the derivatives of the domain integral of Eq. (1) need careful evaluation and generate a Cauchy principal value integral (third integral on the right) together with a free term which contributes to the coefficient g_{ij}.

3 Spatial discretization

The surface Γ is subdivided into a series of boundary elements and the parts of the domain Ω, over which plastic zones are likely to develop, are discretized using internal cells for integrating the inelastic strain contributions.

Also, stresses at boundary nodes are calculated employing the interpolated displacements and tractions over each boundary element as seen in Telles (1983).

Equation (1) therefore leads to

$$\mathbf{H}\dot{\mathbf{u}} = \mathbf{G}\dot{\mathbf{p}} + \mathbf{Q}\dot{\boldsymbol{\sigma}}^{\mathbf{p}} \quad (3)$$

and computation of stresses at selected boundary nodes and internal points (here using Eq. (2)) can be carried out by

$$\dot{\boldsymbol{\sigma}} = \mathbf{G}'\dot{\mathbf{p}} - \mathbf{H}'\dot{\mathbf{u}} + \mathbf{Q}^*\dot{\boldsymbol{\sigma}}^{\mathbf{p}} \quad (4)$$

where matrices **H**, **H'**, **Q**, etc. are classical boundary element matrices. Note that matrix $\mathbf{Q}^*$ also includes the contributions of the free coefficient g_{ij}.

After the application of the displacement and traction boundary conditions, Eqs. (3) and (4) can be written as

$$\mathbf{A}\dot{\mathbf{y}} = \dot{\mathbf{f}} + \mathbf{Q}\dot{\boldsymbol{\sigma}}^{\mathbf{p}} \quad (5)$$

and

$$\dot{\boldsymbol{\sigma}} = -\mathbf{A}'\dot{\mathbf{y}} + \dot{\mathbf{f}}' + \mathbf{Q}^*\dot{\boldsymbol{\sigma}}^{\mathbf{p}} \quad (6)$$

Equation (5) can then be solved for the boundary unknowns included in vector $\dot{\mathbf{y}}$

$$\dot{\mathbf{y}} = \mathbf{K}\dot{\boldsymbol{\sigma}}^{\mathbf{p}} + \dot{\mathbf{m}} \quad (7)$$

where $\dot{\mathbf{m}}$ represents the elastic solution to the boundary problem. Substituting (7) in (6) and rearranging,

$$\dot{\boldsymbol{\sigma}} = \mathbf{S}\dot{\boldsymbol{\sigma}}^{\mathbf{p}} + \dot{\mathbf{n}} \quad (8)$$

in which vector $\dot{\mathbf{n}}$ represents the elastic solution in terms of stresses and

$$\mathbf{K} = \mathbf{A}^{-1}\mathbf{Q}$$
$$\mathbf{S} = \mathbf{Q}^* - \mathbf{A}'\mathbf{K}$$
$$\dot{\mathbf{m}} = \mathbf{A}^{-1}\dot{\mathbf{f}}$$
$$\dot{\mathbf{n}} = \dot{\mathbf{f}}' - \mathbf{A}'\dot{\mathbf{m}}$$

4 Constitutive equations

The incremental stress-strain relations for inviscid plasticity problems can be written in the form

$$\dot{\sigma}_{ij} = C^{ep}_{ijkl}\dot{\varepsilon}_{kl} \quad (9)$$

Here, C^{ep}_{ijkl} is the fourth-order elastoplastic tangent operator that relates total strain increments with stress increments and is defined as follows:

$$C^{ep}_{ijkl} = C_{ijkl} - \frac{1}{\gamma'}C_{ijmn}a_{mn}a_{op}C_{opkl} \quad (10)$$

where C_{ijkl} is the fourth-order tensor of elastic constants with the following form (δ_{ij} is the Kronecker delta symbol):

$$C_{ijkl} = \frac{2G\nu}{1-2\nu}\delta_{ij}\delta_{kl} + G\left(\delta_{ik}\delta_{jl} + \delta_{il}\delta_{jk}\right)$$

and

$$a_{ij} = \frac{\partial \sigma_e}{\partial \sigma_{ij}}$$

$$\gamma' = a_{ij}C_{ijkl}a_{kl} + H'$$

in which H' is the slope of the uniaxial curve (σ_o) plotted as stress versus plastic strain,

$$H' = \frac{d\sigma_o}{d\varepsilon_e^p}$$

In the above equations σ_e is the equivalent or effective stress defined by the yield criterion and ε_e^p is the equivalent plastic strain. The yield condition is defined by

$$F(\sigma_e, \sigma_0) \equiv \sigma_e - \sigma_0 = 0 \tag{11}$$

Introducing the fictitious "elastic" stress increment

$$\dot{\sigma}_{ij}^e = C_{ijkl}\dot{\varepsilon}_{kl} \tag{12}$$

and the inelastic stress increment that connects $\dot{\sigma}_{ij}^e$ with $\dot{\sigma}_{ij}$

$$\dot{\sigma}_{ij}^p = \frac{1}{\gamma'}C_{ijmn}a_{mn}a_{op}C_{opkl}\dot{\varepsilon}_{kl} = D_{ijop}C_{opkl}\dot{\varepsilon}_{kl} \tag{13}$$

Equation (9) can be rewritten as

$$\dot{\sigma}_{ij} = \dot{\sigma}_{ij}^e - \frac{1}{\gamma'}C_{ijmn}a_{mn}a_{op}\dot{\sigma}_{op}^e \tag{14}$$

which shows that the true stress increments can be computed from the elastic stress in incremental form. In addition, the plastic strain increments $\dot{\varepsilon}_{kl}^p$ can be calculated by the relation

$$C_{ijkl}\dot{\varepsilon}_{kl}^p = \frac{1}{\gamma'}C_{ijmn}a_{mn}a_{op}\dot{\sigma}_{op}^e \tag{15}$$

The work hardening hypothesis is

$$\sigma_e\dot{\varepsilon}_e^p = \sigma_{ij}\dot{\varepsilon}_{ij}^p \tag{16}$$

and the normality principle for associated plasticity can be described as

$$\dot{\varepsilon}_{ij}^p = a_{ij}d\lambda \tag{17}$$

where $d\lambda$ is the plastic multiplier. Substituting Eq. (17) in (16) and rearranging

$$d\lambda = \frac{\sigma_e\dot{\varepsilon}_e^p}{\sigma_{ij}a_{ij}} \tag{18}$$

It is easy to show that $\sigma_{ij}a_{ij}$ is a homogeneous function of degree one and this allows for the application of Euler's theorem as follows

$$\sigma_{ij}a_{ij} = \sigma_e \tag{19}$$

Hence, substituting Eq. (19) in (18)

$$d\lambda = \dot{\varepsilon}_e^p \tag{20}$$

The work hardening hypothesis can therefore be rewritten as

$$\dot{\varepsilon}_{ij}^p = a_{ij}\dot{\varepsilon}_e^p \tag{21}$$

5 Implementation procedures

The stress at any instant can be computed from the stress related to the last change of state and the current stress increment as follows

$$\sigma_{ij}\big|_{now} = \sigma_{ij}\big|_{before} + \Delta\sigma_{ij} \tag{22}$$

and, considering the work hardening hypothesis, the stress increment is

$$\Delta\sigma_{ij} = \Delta\sigma_{ij}^e - \Delta\sigma_{ij}^p = \Delta\sigma_{ij}^e - C_{ijkl}a_{kl}\Delta\varepsilon_e^p \tag{23}$$

where $\Delta\varepsilon_e^p$ is the equivalent plastic strain increment, which can be calculated by solving the general nonlinear consistency equation

$$\sigma_e|_{(\sigma_{ij}+\Delta\sigma_{ij})} = \sigma_e|_{(\sigma_{ij}+\Delta\sigma_{ij}^e)} - C_{ijkl}a_{kl}a_{ij}\Delta\varepsilon_e^p \tag{24}$$

and in this case,

$$a_{ij} = \frac{\partial\, \sigma_e|_{(\sigma_{ij}+\Delta\sigma_{ij}^e)}}{\partial\sigma_{ij}}$$

where $\sigma_e = f(\sigma_{ij} + \Delta\sigma^e_{ij})$ is the equivalent stress considering a pure elastic stress increment.

Equation (23) is achieved by a Taylor series expansion of the true equivalent stress around its value calculated at the last load step plus the pure fictitious "elastic" stress increment. Mathematically, this is shown as

$$\sigma_e|_{(\sigma_{ij}+\Delta\sigma_{ij})} = \sigma_e|_{(\sigma_{ij}+\Delta\sigma^e_{ij})} + \frac{\partial\, \sigma_e|_{(\sigma_{ij}+\Delta\sigma^e_{ij})}}{\partial\varepsilon^p_{ij}}\Delta\varepsilon^p_{ij} \tag{25}$$

Expanding the second term in the right of Eq. (25) leads to

$$\sigma_e|_{(\sigma_{ij}+\Delta\sigma_{ij})} = \sigma_e|_{(\sigma_{ij}+\Delta\sigma^e_{ij})} + \frac{\partial\, \sigma_e|_{(\sigma_{ij}+\Delta\sigma^e_{ij})}}{\partial\sigma_{kl}} \cdot \frac{\partial\sigma_{kl}}{\partial\varepsilon^p_{ij}}\Delta\varepsilon^p_{ij}$$

$$= \sigma_e|_{(\sigma_{ij}+\Delta\sigma^e_{ij})} + a_{kl}\frac{\partial\sigma_{kl}}{\partial\varepsilon^p_{ij}}\Delta\varepsilon^p_{ij} \tag{26}$$

Taking into consideration that the pure elastic stress and the plastic strains are not directly dependent, the following is readily observed:

$$\frac{\partial\sigma_{kl}}{\partial\varepsilon^p_{ij}} = \frac{\partial\sigma^e_{kl}}{\partial\varepsilon^p_{ij}} - \frac{\partial\sigma^p_{kl}}{\partial\varepsilon^p_{ij}} = -\frac{\partial\sigma^p_{kl}}{\partial\varepsilon^p_{ij}} = -C_{klij} = -C_{ijkl} \tag{27}$$

Substituting Eq. (27) in (26), leads to

$$\sigma_e|_{(\sigma_{ij}+\Delta\sigma_{ij})} = \sigma_e|_{(\sigma_{ij}+\Delta\sigma^e_{ij})} - C_{ijkl}a_{kl}\Delta\varepsilon^p_{ij} \tag{28}$$

Considering the hypothesis of work hardening, Eq. (28) becomes Eq. (24). Such an equation includes as a particular case the consistency equation presented by Simo and Taylor (1985) based on von Mises' criterion and used in a BEM context by Bonnet and Mukherjee (1996), but is here in a general form without any restrictions about yield criterion.

In order to compute the elastic stress increments in the process, the free term g_{ij} can be substituted by $\overline{g}_{ij} = g_{ij} + \delta_{ij}$, leading to the substitution of matrix $\mathbf{S}$ by $\overline{\mathbf{S}} = \mathbf{S} + \mathbf{I}$, where $\mathbf{I}$ is the identity matrix. Equation (8) can now be rewritten, in incremental form, as

$$\overline{\mathbf{S}}(\Delta\boldsymbol{\sigma}^{\mathbf{e}} - \Delta\boldsymbol{\sigma}) + \Delta\mathbf{n} - \Delta\boldsymbol{\sigma}^{\mathbf{e}} = \mathbf{0} \tag{29}$$

Which, according with Eq. (14), allows for the following definition

$$\Re(\Delta\boldsymbol{\sigma}^{\mathbf{e}}) \equiv \overline{\mathbf{S}}\mathbf{D}\Delta\boldsymbol{\sigma}^{\mathbf{e}} + \Delta\mathbf{n} - \Delta\boldsymbol{\sigma}^{\mathbf{e}} \approx \mathbf{0} \tag{30}$$

where $\Re(\Delta\boldsymbol{\sigma}^{\mathbf{e}})$ is the residual and $\mathbf{D}$ is a matrix of the form

$$\mathbf{D} = \begin{bmatrix} [\mathbf{d}] & & & \mathbf{0} \\ & [\mathbf{d}] & & \\ & & \ddots & \\ \mathbf{0} & & & [\mathbf{d}] \end{bmatrix} \tag{31}$$

Here, the sub-matrices $\mathbf{d}$ of the diagonal play the role of D_{ijop}, in point-wise fashion, in Eq. (13). The nonlinear Eq. (30) can now be solved using Newton's method. In this case, the correction $\boldsymbol{\delta\sigma}^{\mathbf{e}} = \boldsymbol{\Delta\sigma}^{\mathbf{e}}_{\mathbf{n+1}} - \boldsymbol{\Delta\sigma}^{\mathbf{e}}_{\mathbf{n}}$, which is the difference between pure elastic stress increments for iterations "n" and "$n+1$" , solves

$$\left[\overline{\mathbf{S}}\mathbf{D} - \mathbf{I}\right]\boldsymbol{\delta\sigma}^{\mathbf{e}} = \Re(\boldsymbol{\Delta\sigma}^{\mathbf{e}}) \tag{32}$$

where the term in square brackets define a tangent matrix, first seen in Telles (1985), also called global tangent operator by Poon, Mukherjee and Bonnet (1998) and Paulino and Liu (2001). Note that the components of the global tangent operator which multiplies the corrections $\delta\sigma^e_{ij}$ related to elastic nodes are the same as the identity tensor, i.e., if no plasticity is developing, $\mathbf{d} = \mathbf{0}$. This fact is of great relevance to the performance of the implementation, since the system of equations presented in Eq. (32) must be solved once per iteration.

The convergence criterion, measured in terms of the discrete residual norm for all nodes, is defined as

$$\left\|\Re(\Delta\sigma^e_{ij})\right\| \overset{def}{=} \sqrt{\frac{\sum\left(\Re(\Delta\sigma^e_{ij})\right)^2}{4N}} \leq TOL \tag{33}$$

The structure of the implicit algorithm is the following:

1. For $0 \leq n \leq (N_T - 1)$:
2. Compute $\boldsymbol{\Delta n} = \omega\mathbf{n}$
3. Initialize $\boldsymbol{\Delta\sigma}^{\mathbf{e}} = \boldsymbol{\Delta n}$

Iterative solution of Eq. (30):

2.1 $i = 0$

2.2 Compute residual $\Re(\boldsymbol{\Delta\sigma}^{\mathbf{e}})$ from Eq. (30).

2.3 Test the convergence condition on Eq.(33) is satisfied: if YES, go to 3.

2.4 $i := i + 1$

2.5 Compute the local tangent operators for all nodes and determine which ones present plastic and elastic behavior.

2.6 Set up the global tangent operator.

2.7 Solve equation (32).

2.8 Update: $\Delta\boldsymbol{\sigma}^{\mathbf{e}} = \Delta\boldsymbol{\sigma}^{\mathbf{e}} + \delta\boldsymbol{\sigma}^{\mathbf{e}}$

2.9 Go to 2.2 for new iteration

3. Update:

$\varepsilon_e^p = \varepsilon_e^p + \Delta\varepsilon_e^p$

$$\boldsymbol{\sigma} = \boldsymbol{\sigma} + (\mathbf{I} - \mathbf{D})\,\Delta\boldsymbol{\sigma}^{\mathbf{e}} \tag{34}$$

where ω is the load increment percentage given in terms of load at first yield.

It is worth noticing that the application of Eq. (34) has the same effect of the radial return algorithm (RRA) presented in Simo and Taylor (1985), Bonnet and Mukherjee (1996), Poon, Mukherjee and Bonnet (1998) and Paulino and Liu (2001). Here, this denomination is no longer adequate since it comes from a particularization for von Mises' yield criterion, not as general as discussed here.

6 Results

In order to verify the accuracy of the technique presented, the following examples are discussed:

- A perforated plate under uniform tension,
- A rectangular block compressed by two opposite rigid punches,
- A flexible strip footing under uniform loading.

Even though internal cells are needed only where plastic strains are likely to develop, for academic reasons, in some examples, the internal mesh includes the complete domain. Symmetry with respect of the two axes is considered in the first two examples and, in the last example, symmetry is considered only with respect to the y-axis.

The results presented here are compared with the ones obtained with a well-established (see Telles (1983)) explicit initial stress BEM technique.

6.1 Perforated plate

The first problem analyzed by the presented technique is a plane stress analysis of a perforated steel plate under uniform tension. Its geometry and the discretization of its upper right quadrant are shown, respectively, in Figs. 1 and 2. The yield criterion adopted is von Mises'. The problem characteristics are presented in Table 1.

Table 1 : problem characteristics - perforated plate

Item	Quantity
Applied load (q)	11.5 kgf/mm^2
Young modulus (E)	7000 kgf/mm^2
Tangent modulus (E_T)	217 kgf/mm^2
Yield stress (Y)	24.3 kgf/mm^2
Poisson ratio (ν)	0.2
Load increment	10.0%
Boundary nodes	25
Internal points	11
Boundary elements	22
Internal cells	29

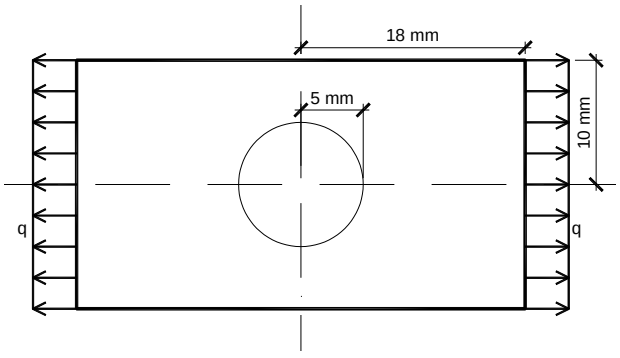

Figure 1 : plate problem geometry

The plastic zone has evolved in the same way on both, implicit and explicit methods. These results are presented in Fig. 3. Other result analyzed is the σ_y-stress over points located at the x-axis, which is presented in Fig. 4. The starting of plasticity was achieved with about 50% of the applied load.

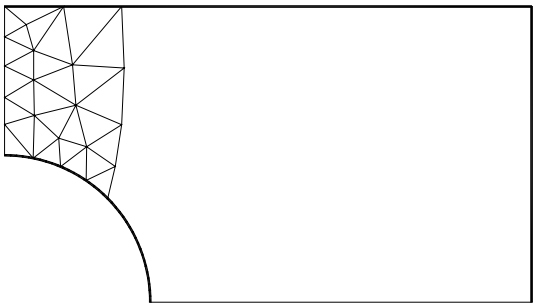

Figure 2 : problem discretization

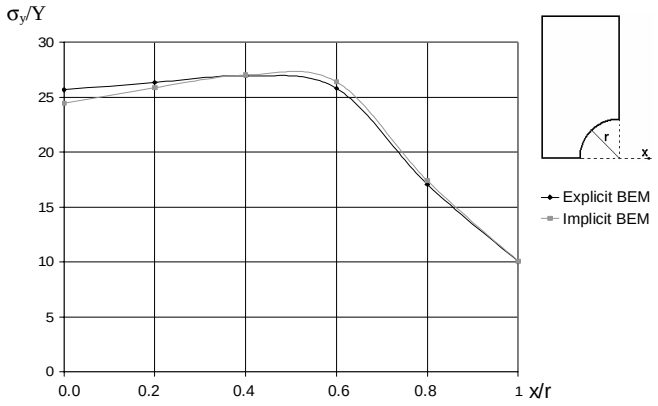

Figure 4 : σ_y-stress at x-axis

Table 2 : number of iterations per load increment – perforated plate problem

Method	Percentage of applied load									
	55	60	65	70	75	80	85	90	95	100
Explicit	9	9	9	9	9	22	22	36	31	44
Implicit	4	4	4	4	4	5	5	5	6	6

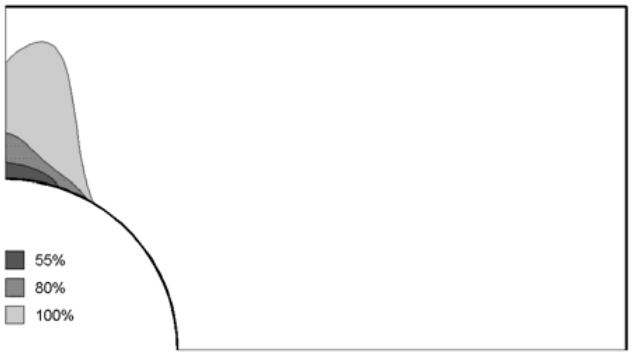

Figure 3 : plastic deformation zone at certain percentages of applied load;

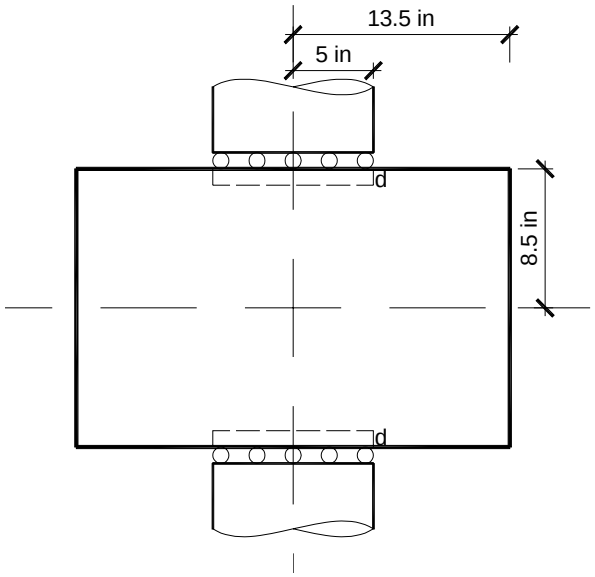

Figure 5 : block geometry

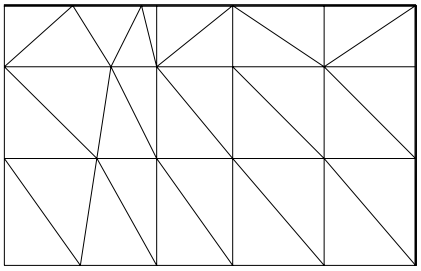

Figure 6 : problem discretization

In order to present a more illustrative comparison between the two methods, Table 2 shows the number of iterations per load increment.

6.2 Punch problem

The second problem studied is a rectangular block compressed by two opposite rigid punches. Its geometry and upper right quadrant discretization are shown in Figs. 5 and 6. The yield criterion adopted in this problem is von Mises'. The problem characteristics are presented in Table 3.

Table 3 : problem characteristics – punch problem

Item	Quantity
Imposed displacement (d)	0.05 in
Young modulus (E)	10^7 psi
Tangent modulus (E_T)	-
Yield stress (Y)	13000 psi
Poisson ratio (ν)	0.33
Load increment	10.0%
Boundary nodes	12
Internal points	15
Boundary elements	9
Internal cells	31

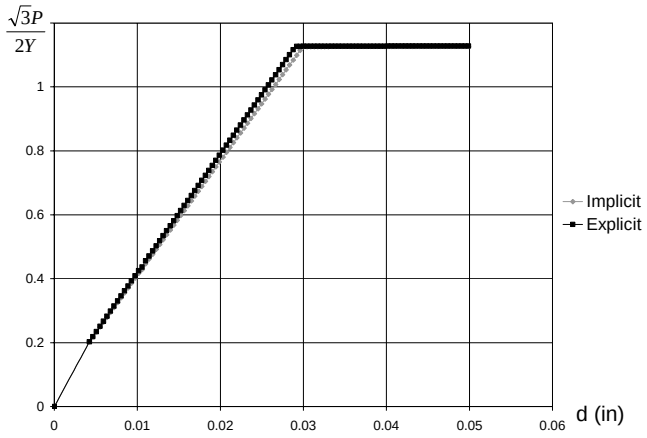

Figure 7 : mean pressure vs. punch displacement

Table 4 : iterations per load increment – punch problem

Method	Percentage of applied displacement						
	16.5	23.0	29.5	36.0	42.5	49.0	55.5
Explicit	32	48	55	55	55	55	58
Implicit	22	28	39	38	32	35	43
Method	Percentage of applied displacement						
	62.5	69.0	75.5	82.0	88.5	95.0	101.5
Explicit	65	67	70	70	74	75	75
Implicit	37	32	66	32	41	36	40

The relation between the mean pressure applied by the rigid punch and its prescribed displacement is shown in Fig. 7. The evolution of the plastic zone (the same on both methods) is presented in Fig. 8.

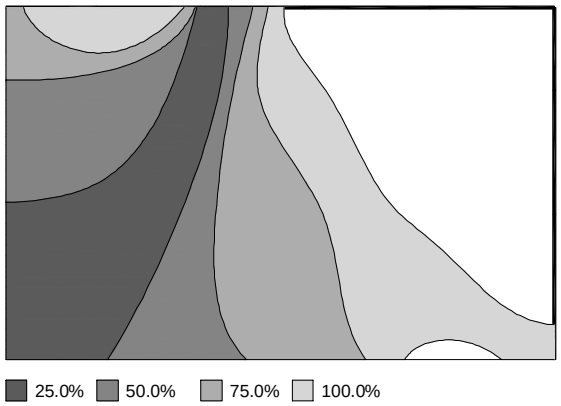

Figure 8 : plastic zone development at certain percentages of applied displacement;

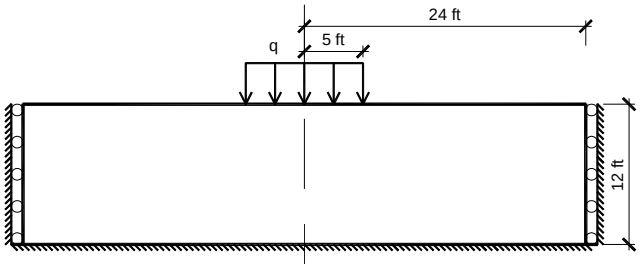

Figure 9 : strip footing geometry

The accumulated number of iterations corresponding to every 6.5% of load increment is presented in Table 4. Plasticity starts to develop with 11% of the imposed displacement in this problem.

6.3 Strip footing

The last example presented is a plane strain analysis of a flexible strip footing under uniform loading. Its geometry and the discretization are seen in Figs. 9 and 10. The BEM formulation for this problem adopted a half-space fundamental solution found in Telles (1983). The yield criterion adopted in this problem is Mohr-Coulomb's. The problem characteristics can be seen in Table 5. The results plotted in Fig. 11 are the relation between the displacement of the node at the center of the loading and the applied load. The evolution of the plastic zone in the problem is shown in Fig. 12 for both methods. The growth of the plastic zone follows the same path up to the

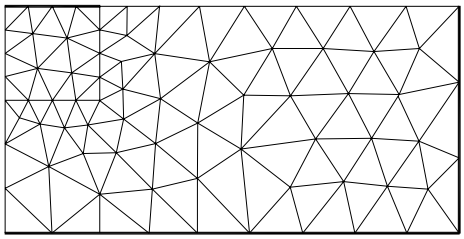

Figure 10 : problem discretization

Table 5 : problem characteristics – strip footing

Item	Quantity
Applied load (q)	180 psi
Young modulus (E)	30000 psi
Tangent modulus (E_T)	-
Poisson ratio (ν)	0.3
Cohesion	10.0 psi
Friction angle	20º
Load increment	12.5%
Boundary nodes	19
Internal points	59
Boundary elements	16
Internal cells	121

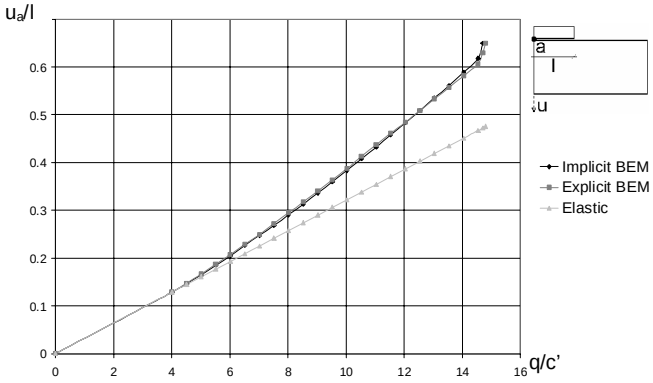

Figure 11 : displacement of the center of the loading vs. applied load

last converged solution.

The accumulated number of iterations corresponding to a certain percentage of load is presented in Table 6. Plasticity starts to develop with 25% of the applied load in this problem.

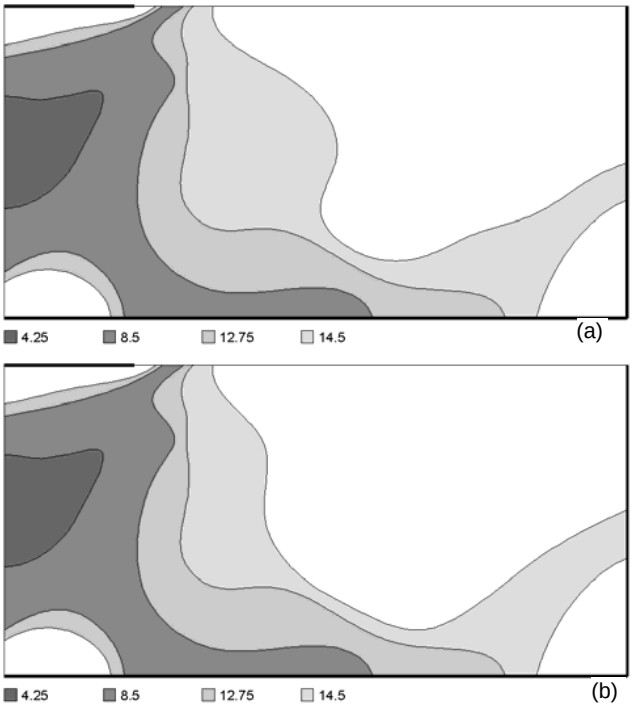

Figure 12 : plastic zone at different applied loads – (a) explicit BEM; (b) implicit BEM.

Table 6 : number of iterations per load increment – strip footing problem

Method	Percentage of applied load				
	40	55	70	85	100
Explicit	93	182	197	413	813
Implicit	18	35	37	40	33

7 Conclusions

The main goal of this work is to introduce a proper criterion-independent tangent operator implicit technique for elastoplastic problems with boundary elements, generalizing what was previously presented using just J_2-type yield criteria.

The results obtained with the multi-criteria implicit technique show its accuracy and the observed reduction in the number of iterations per load step has been substantial in

comparison with the explicit counterpart.

References

Bonnet, M.; Mukherjee, S. (1996) Implicit BEM formulations for usual sensitivity problems in elastoplasticity using the consistent tangent operator concept, *Int. J. Solids Struct*., vol. 33, pp. 4461-4480.

Hatzigeorgiou, G. D.; Beskos, D. E. (2002): Dynamic response of 3-D damaged solids and structures by BEM, *CMES: Computer Modeling in Engineering & Sciences*, vol. 3, no. 6, pp. 791-801.

Jin, H.; Runesson, K.; Mattiasson, K. (1989): Boundary element formulation in finite deformation plasticity using implicit integration, *Comput. Struct.*, vol. 31, pp. 25-35.

Leu, L. J.; Mukherjee, S. (1994): Sensitivity analysis of hyperelastic-viscoplastic solids undergoing large deformations, *Comput. Mech.*, vol. 15, pp. 101-116.

Liu, C. S.; Chang, C. W. (2004): Lie group symmetry applied to the computation of convex plasticity constitutive equation, *CMES: Computer Modeling in Engineering & Sciences*, vol. 6, no. 3, pp. 277-294.

Okada, H.; Rajiyah, H.; Atluri, S. N. (1990): Full tangent stiffness field-boundary-element formulation for geometric and material non-linear problems of solid mechanics, *Int. J. Num. Methods in Engng.*, vol. 29, pp. 15-35.

Paulino, G. H.; Liu, Y. (2001): Implicit consistent and continuum tangent operators in elastoplastic boundary element formulations, *Comput. Methods Appl. Mech. Engrg*., vol. 190, pp. 2157-2179.

Poon, H.; Mukherjee, S.; Bonnet, M. (1998): Numerical implementation of a CTO-based implicit approach for the BEM solution of usual and sensitivity problems in elastoplasticity, *Engrg. Anal. Boundary Elem.,* vol. 22, pp. 257-269.

Riccardella, P. C. (1973): An implementation of the boundary integral technique for planar problems in elasticity and elastoplasticity, SM-73-10, Dept. Mech. Engng., Carnegie Mellon Univ., Pittsburg.

Simo, J. C.; Taylor, R. L. (1985): Consistent tangent operators for rate-independent elastoplasticity, *Comput. Methods Appl. Mech. Engrg*., vol. 48, 101-118.

Telles, J. C. F. (1983): The boundary element method applied to inelastic problems. In: *Lecture Notes in Engineering*, vol.1, Springer-Verlag, Berlin Heidelberg.

Telles, J. C. F. (1985): On inelastic analysis algorithms for boundary elements. In: T. Cruse, A. Pifko, H. Arnen, (eds.) *Winter Annual Meeting of the ASME, AMD Vol. 72*, Miami, USA, pp. 35-44.

Telles, J. C. F.; Carrer, J. A. M. (1988): Implicit solution techniques for inelastic boundary element analysis. 10^{th} *BEM*, vol. 3, pp. 3-15.

Telles, J. C. F.; Carrer, J. A. M. (1991): Implicit procedures for the solution of elastoplastic problems by the boundary element method. *Math. Comput. Model.,* vol. 15, pp. 303-311.

Telles, J. C. F.; Carrer, J. A. M. (1994): Static and transient dynamic nonlinear stress analysis by the boundary element method with implicit techniques. *Engrg. Anal. Boundary Elem.,* vol. 14, pp. 65-74.